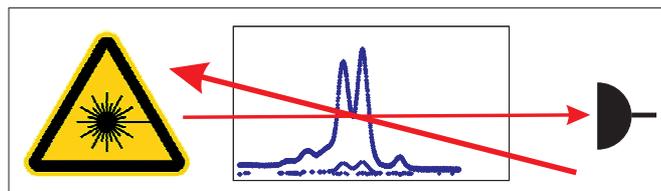# Doppler-Free Saturation Spectroscopy

Thomas Rieger and Thomas Volz

Max-Planck-Institut für Quantenoptik, Garching

1 Introduction

With the advent of the laser in the 1960s, precision spectroscopy of atoms and molecules became possible. The laser, being a very narrow, tunable and coherent light source, allowed to resolve features in atomic and molecular spectra with an unprecedented resolution and accuracy, which led to a better understanding of the structure of atoms and molecules. Precision spectroscopy became a very active field and within a short time, a wide range of different spectroscopic techniques were developed. A good review is for instance the article [1] written by T. W. Hänsch, A. L. Schawlow and G. W. Series, which gives an overview of precision spectroscopy of atomic hydrogen. Many of the basic principles and techniques can be understood from this article and are still not outdated. Another very good and comprehensive introduction on a more detailed basis is given in the book "Laser Spectroscopy" by W. Demtröder [2], one of the pioneers of the field.
Laser spectroscopy also paved the way towards all the exciting developments that took place in the past two decades in the field of laser cooling and trapping of atoms which culminated in 1995 with the realisation of Bose-Einstein condensation in alkali gases [3]. In all the labs dealing with laser cooling and trapping of atoms, the technique of Doppler-free saturated absorption spectroscopy is frequently used as a tool for locking the lasers to particular atomic lines. In this graduate-student lab experiment, this technique is introduced in theory and experiment.

2 Saturation Spectroscopy

2.1 Qualitative Picture for Two-Level Atoms

The experimental setup for doing Doppler-free saturation spectroscopy is shown in Fig. 1. Two counter-propagating laser beams derived from a single laser beam are sent through an atomic vapour cell. While the "pump" beam has a high intensity and serves to bleach the atomic gas, i.e. to make the gas transparent, the transmittance of the "probe" beam through the atomic vapour is recorded with a photodiode and gives the actual spectroscopic signal. Typically the probe beam has a factor of ten smaller intensity.

In order to understand what kind of signals one can expect, let us for simplicity consider (fictitious) atoms with only two internal states, the ground
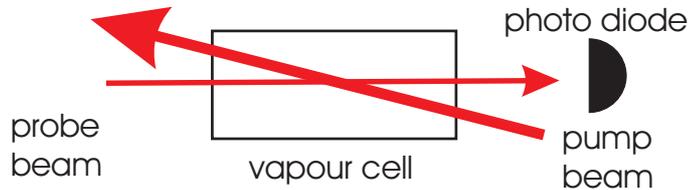
Figure 1: Basic experimental arrangement for saturation spectroscopy.

state $|g\rangle$ and the excited state $|e\rangle$. Then, the kind of signals one would get when scanning the laser frequency are shown in Fig. 2. If the pump beam is blocked and only the probe beam goes through the vapour cell, one obtains a simple absorption line exhibiting a strong Doppler broadening. Note the typical Gaussian absorption profile. Typically, the Doppler broadening at room temperature exceeds the natural linewidth, that is the intrinsic frequency width of an atomic transition, by two orders of magnitude.

Problem 1 Derive a formula for the Doppler-broadening of atomic transitions in terms of the resonance frequency ν_0, the temperature T and atomic mass m. What is the Doppler broadening for the D-lines in rubidium ($\nu_0 \approx 3.84 \cdot 10^{14}$Hz) at room temperature? The natural linewidth of the transition is $\Gamma \approx 6$Mhz.

Now, if in addition the pump beam is sent through the vapour cell, a very narrow spike appears in the probe-beam signal at the resonance frequency $\nu = \nu_0$ of the atomic transition. This is the so-called Lamb dip, named after W. Lamb who first recognized the huge potential of saturation spectroscopy.

The reason for this spike to show up is the following: only for atoms having zero velocity along the long axis of the vapour cell the two counter-propagating laser beams have the same frequency. Atoms moving e.g. to the right see the frequency of the pump beam shifted into the blue whereas for the same atoms the probe beam is red-shifted. Hence, whenever atoms with $v \neq 0$ see the probe beam shifted into resonance due to the Doppler effect, at the same time the pump beam is shifted further away from resonance.

Atoms at zero velocity, however, do see both the pump and the probe beam. The high intensity or equivalently the high photon flux in the pump beam, leads to a high absorption rate. The atoms absorb photons from the pump beam and undergo a transition to the excited state, from where
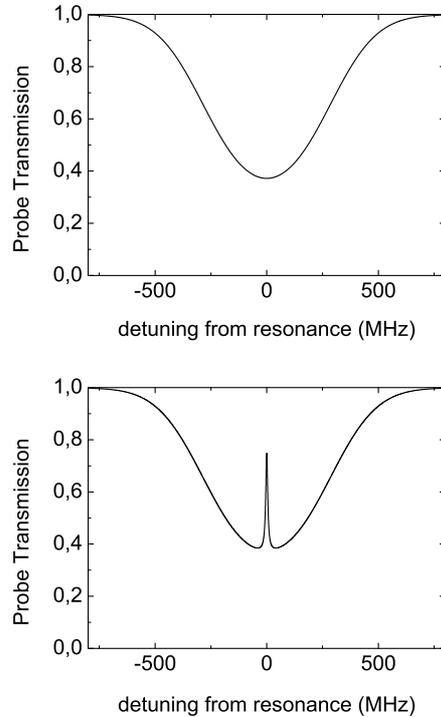
Figure 2: Transmission signal for a probe beam without (a) and with (b) an intense pump beam present.

they eventually fall back to the ground state by spontaneous emission. If the pump-beam intensity is high enough, the ground state is significantly depleted and therefore the absorbance of the probe beam is reduced compared to the case without pump beam: a spike appears in the transmission spectrum of the probe beam. Note, that for infinite intensity of the pump beam, on average half of the atoms would be in the excited state and no probe absorption would occur (next section). This is called "saturation" of the atomic transition. Hence, the name "saturation spectroscopy".

The last remark of this section concerns the width of the Lamb dip. Obviously the dip is much narrower than the Doppler width. If the intrinsic frequency width (linewidth) of the laser used in the experiment is small

enough, the observed width of the Lamb dip can be as small as the natural linewidth of the atomic transition.

2.2 Quantitative Picture for Two-Level Atoms

It is fairly straightforward to calculate a crude saturated-absorption spectrum for a two-level atom. A lot of the underlying physics can be understood from such a model.

Optical Depth
The intensity I of a single weak laser beam propagating through a vapour cell changes according to Beer's law as

$$dI/dx = -\alpha I , \tag{1}$$

where $\alpha = \alpha(\nu)$ is the frequency-dependent extinction coefficient. In the case of a single weak beam, to a good approximation α does not depend on position. Then, the overall transmission through the vapour cell of length l is given by

$$I_{out} = I_{in}e^{-\alpha(\nu)l} = I_{in}e^{-\tau(\nu)} , \tag{2}$$

where $\tau(\nu) = \alpha(\nu)l$ is called the optical depth. The contribution from one velocity class of atoms $(v, v + dv)$ to $\tau(\nu)$ can be written as

$$d\tau(\nu, v) = l\sigma(\nu, v)dn(v) . \tag{3}$$

The absorption coefficient $\sigma(\nu, v)$ has a Lorentzian profile with natural linewidth Γ and a Doppler-shifted resonance frequency

$$\sigma(\nu, v) = \sigma_0 \frac{\Gamma^2/4}{(\nu - \nu_0 + \nu_0 v/c)^2 + \Gamma^2/4} . \tag{4}$$

σ_0 is the on-resonance absorption cross section. In general, it depends on the character of the atomic transition (dipole, quadrupole, etc.) and the polarization of the incident light (see e.g. Ref.[4]).
The fraction of atoms $dn(v)$ belonging to a certain velocity class follows a Boltzmann distribution

$$dn(v) = n_0 \sqrt{\frac{m}{2\pi k_B T}} \, e^{-mv^2/2k_B T} dv . \tag{5}$$

with $n_0 = N/V$ being the density of atoms in the vapour cell. Putting everything together, we obtain the differential contribution to the optical depth for laser frequency ν and atomic velocity v

$$d\tau(\nu, v) = \frac{2}{\pi} \frac{\tau_0}{\sigma_0 \Gamma} \frac{\nu_0}{c} \sigma(\nu, v) e^{-mv^2/2k_B T} dv \ , \tag{6}$$

where the overall normalization is chosen such that τ_0 is the optical depth at resonance, i.e. $\tau_0 = \int d\tau(\nu_0, v)$ with the integral over all velocity classes.

Problem 2: Under the assumption that the natural linewidth of the atomic transition is much smaller than the Doppler width, i.e. $\Gamma \ll \Delta_D$, derive an expression for the on-resonance optical depth τ_0 in terms of σ_0, n_0, Γ and Δ_D. Discuss your result.

For the situation of Doppler-free saturation spectroscopy we need to account for the effect of the additional strong pump beam. Due to the presence of this strong laser beam a significant part of the atoms in the vapour cell will be in their excited state. And since atoms can only absorb light when they are in the ground state, we need to insert a factor $\frac{N_g - N_e}{N}$ in the above formula (6), describing the difference between excited state population N_e and ground state population N_g.

Rate Equations
The populations in the two states follow the rate equations

$$\begin{aligned} \dot{N}_g &= \Gamma N_e - \sigma \Phi (N_g - N_e) \tag{7} \\ \dot{N}_e &= -\Gamma N_e + \sigma \Phi (N_g - N_e) \ , \tag{8} \end{aligned}$$

where the first term in each equation stems from spontaneous emission and the second term from stimulated processes. $\Phi = I/h\nu$ is the incident photon flux. Next, N_g can be eliminated using $N_g + N_e = N = const.$ Then, all the physics is contained in the equation for N_e

$$\dot{N}_e = -\left(\Gamma N_e + 2\sigma \Phi\right) N_e + \sigma \Phi N \ . \tag{9}$$

This differential equation is solved by

$$N_e(t) = \left[\Gamma N_e(0) - \frac{N\sigma\Phi}{\Gamma + 2\sigma\Phi}\right] e^{-(\Gamma + 2\sigma\Phi)t} + \frac{N\sigma\Phi}{\Gamma + 2\sigma\Phi} \ . \tag{10}$$

Several examples of this general solution are shown in Fig. 3: In the case of
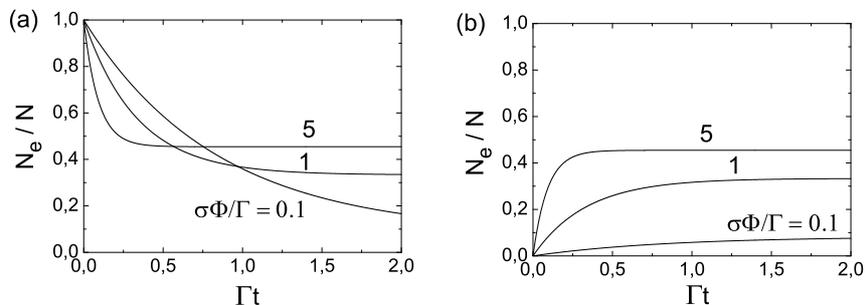
Figure 3: Excited-state population N_e as a function of time. Fig. (a) shows an exponential decay of population with $N_e(t = 0) = N$, in Fig. (b) the population in N_e increases exponentially in time. In any case the population in the excited state satisfies $N_e < N/2$ for long times.

no radiation field present, the system exhibits a purely exponential decay

$$N_e(t) = N_e(0)e^{-\Gamma t} \ . \tag{11}$$

With a weak light source present, i.e. $\sigma\Phi \ll \Gamma$, and with initially all population in the ground state, the population in the excited state increases as

$$N_e(t) = \frac{N\sigma\Phi}{\Gamma} \left[1 - e^{-\Gamma t}\right] \ , \tag{12}$$

and after a time Γ^{-1} reaches a very small steady-state population $N\sigma\Phi/\Gamma \ll N$. However, in the experiment, we are dealing with a very strong pump laser. For $\sigma\Phi \gg \Gamma$, we get a fully saturated transition

$$N_e(t) = \left[N_e(0) - N/2\right] e^{-2\sigma\Phi t} + N/2 \ \rightarrow N/2 \ . \tag{13}$$

Here, saturation means, that half the population is in the excited state. Even for infinite power, it is therefore not possible to have more than half of the atoms in the excited state - at least for a two-level system. Lasers rely on population inversion and therefore involve at least three atomic levels.

6

Another effect well-known in laser spectroscopy is power broadening, which is also present in the steady-state solutions of Eqn.(10). In the limit $(\Gamma + 2\sigma\Phi)t \gg 1$, we get

$$\frac{N_e(\infty)}{N} = \frac{\sigma\Phi}{\Gamma + 2\sigma\Phi} \ . \tag{14}$$

Using expression Eqn. (4) and writing $\Delta\nu = (\nu - \nu_0 - \nu_0 v/c)$ (note the minus sign, due to the opposite Doppler shift for the pump beam compared to the probe beam), we can rearrange that expression and obtain

$$\frac{N_e(\infty)}{N} = \frac{\sigma_0\Phi\Gamma/4}{\Delta\nu^2 + \Gamma^2/4 + \sigma_0\Phi\Gamma/2} \ . \tag{15}$$

This is a Lorentzian whose "power-broadened" half width now depends on the incident photon flux

$$\Delta_{1/2} = \Gamma/2 \left(1 + \frac{2\sigma_0\Phi}{\Gamma}\right)^{1/2} \ . \tag{16}$$

Introducing the saturation parameter $s = \Phi/\Phi_{sat}$, where $\Phi_{sat} = \Gamma/2\sigma_0$, we obtain a very convenient formula for the population in the excited state

$$N_e = \frac{s/2}{1 + s + 4\Delta^2/\Gamma^2} \ . \tag{17}$$

With this expression for the excited-state population N_e in terms of detuning Δ and saturation parameter s, we have all the ingredients we need to calculate a simple saturated-absorption spectrum for a two-level atom.

Let us conclude this section by noting that the saturation intensity I_{sat} can be expressed as [4]

$$I_{sat} = 2\pi^2 hc\Gamma/3\lambda^3 \ . \tag{18}$$

For the D_2 line in ^{87}Rb with a natural linewidth of $\Gamma = 6$ MHz, the saturation intensity is $I_{sat} \approx 1.65$ mW/cm^2.

Calculated Saturated-Absorption Spectra

In the last two paragraphs we have seen, that a saturated absorption spectrum is basically determined by two externally adjustable parameters, namely the pump intensity and the on-resonance optical depth. Assuming a fixed
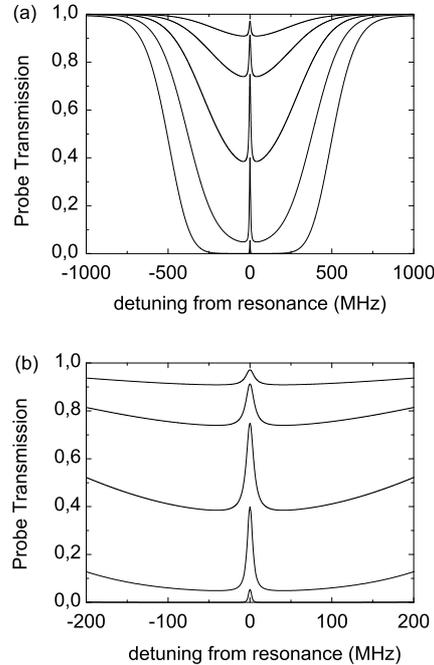
Figure 4: Probe transmission as a function of laser frequency for different vapour densities. Fig. (b) is a zoom into the region around ν_0: for very high densities the saturated-absorption peak vanishes.

temperature and choosing a particular atomic species the latter is proportional to the vapour density inside the cell (also see Problem 1). Fig. 4 shows absorption spectra for different densities in the cell. At low densities, the probe absorption is weak and shows a Gaussian profile. When increasing the density, the absorption increases and the profile gets broader and deeper. For even higher densities, the depth is saturated but the width further increases, the profile looses its Gaussian shape. The density of absorbing atoms is so high, that even far from resonance the probe gets absorbed almost completely. On resonance the absorption is reduced due to the effect of the strong pump beam and we recognize the saturated absorption feature. For increasing density, however, this feature becomes smaller and smaller (com-

pare Fig. 4b). Increasing the atomic density and holding the pump beam intensity fixed, corresponds to an increase in the absolute number of atoms in the ground state: the absorption at $\nu = \nu_0$ increases. In Fig. 5 the density
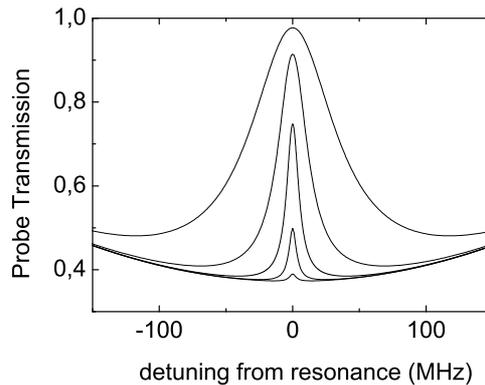

Figure 5: Saturated-absorption peak at $\nu = \nu_0$ for fixed vapour density and varying pump beam intensity. The effect of power broadening is clearly visible.

is fixed and the intensity of the pump beam is varied. For higher intensities, the Lamb dip becomes higher and broader: the pump beam saturates and power-broadens the atomic transition.

3   Multilevel Atoms - Alkalis

Alkali atoms are the workhorse in many of today's experiments dealing with the trapping, cooling and manipulation of atoms. Their popularity has multiple reasons. Most important is their relatively simple hydrogen-like level structure due to a single valence electron in the outer shell. In contrast to hydrogen, however, the transition frequency from the ground to the first excited state typically lies in the visible or near-infrared part of the spectrum, which can be conveniently accessed by relatively cheap and reliable lasers that are commercially available. In this experiment, for example, rubidium is used with a transition frequency at 780 nm, for which light can be generated by standard diode lasers (see for example Refs. [4, 5]).

3.1 Fine-Structure Splitting

In the case of rubidium the inner four electronic shells are filled, and only the single outer (5s) valence electron determines the angular momentum configuration of the atom. The state of the electron is completely described by its orbital angular momentum $\vec{L}$ and its spin $\vec{S}$. These two angular momenta couple in the usual way to form the total angular momentum J of the electron. Hence, J can take the values $|L - S| \leq J \leq |L + S|$. Responsible for the coupling is the so-called spin-orbit interaction, which can be written as $V_{so} = A_{fs}\vec{L} \cdot \vec{S}$. It is a relativistic effect and can be readily derived from the Dirac equation for spin-1/2 particles. Simply speaking, the spin-orbit coupling is nothing else but the magnetic interaction energy of the electronic spin in the magnetic field due to the relative motion of nucleus and electron. For details, see any good book on (relativistic) quantum mechanics. The spin-orbit coupling leads to the so-called fine-structure splitting for different values of the total angular momentum $\vec{J}$.

For the alkali atoms the electronic states are fully specified in the so-called Russell-Saunders notation $n^{(2S+1)}L_J$, where n denotes the principal electronic quantum number. Hence, $n = 5$ in the case of Rb, and its ground state is given by $5^2S_{1/2}$. The fine-structure splitting between the first excited states $5^2P_{1/2}$ and $5^2P_{3/2}$ is 7123 GHz.

3.2 Hyperfine-Structure Splitting

If the rubidium nucleus carried no spin, the $5^2S_{1/2}$, $5^2P_{1/2}$ and $5^2P_{3/2}$ energy levels would be singlets with no external fields applied. However, this is not true; there are two natural isotopes of rubidium: ^{87}Rb with a nuclear spin of $I = 3/2$ and ^{85}Rb with $I = 5/2$ and a higher abundance level of 72%. The non-vanishing nuclear spins have magnetic and (electric) quadrupolar moments associated with them, leading to the so-called hyperfine splitting of the atomic energy levels.

The first contribution to the hyperfine splitting is the energy of the nuclear magnetic (dipole) moment $\vec{\mu}_{nucl}$ in the magnetic field $\vec{B}_{el}$ generated by the valence electron at the position of the nucleus

$$H_{magn}^{hf} = -\vec{\mu}_{nucl} \cdot \vec{B}_{el}. \tag{19}$$

Since $\vec{\mu}_{nucl}$ is proportional to the nuclear spin $\vec{I}$ and $\vec{B}_{el}$ is proportional to the total angular momentum of the valence electron $\vec{J}$, H_{magn}^{hf} can be rewritten as

$\alpha \vec{I} \cdot \vec{J}$. The parameter α is called the magnetic hyperfine structure constant and has units of energy, that is $\vec{I}$ and $\vec{J}$ are taken to be dimensionless.

A second contribution to the hyperfine splitting arises from the electrostatic interaction between the valence electron and the non-vanishing electric quadrupole moment of the nucleus. This interaction can be reexpressed in terms of the nuclear and electron angular momenta $\vec{I}$ and $\vec{J}$ as follows [3]

$$H^{hf}_{quadr} = \frac{\beta}{2I(2I-1)J(2J-1)}[3(\vec{I}\vec{J})^2 + \frac{3}{2}(\vec{I}\vec{J}) - I(I+1)J(J+1)], \quad (20)$$

where -in analogy to the magnetic case- β is called the electric quadrupole interaction constant and has units of energy.

These two interactions lead to a coupling of the nuclear angular momentum $\vec{I}$ and the electron angular momentum $\vec{J}$ to the total angular momentum $\vec{F} = \vec{I} + \vec{J}$, where F can take any value between $|J - I|$ and $J + I$. Associated with the coupling is a splitting into hyperfine levels, which are labelled by the hyperfine quantum number F. Electric dipole transitions between hyperfine levels must obey the selection rules

$$\Delta L = \pm 1 \quad (21)$$
$$\Delta F = 0, \pm 1 \ (not \ 0 \to 0). \quad (22)$$
$$\Delta J = 0, \pm 1 \quad (23)$$

Using the definition for $\vec{F}$ and forming $\vec{F} \cdot \vec{F}$, it is possible to write $\vec{I} \cdot \vec{J} = [F(F+1) - J(J+1) - I(I+1)]/2 =: C/2$. Hence, for given J and I, the frequencies ν_F of the various hyperfine levels are given by

$$\nu_F = \nu_J + \frac{AC}{2} + B[\frac{3C(C+1) - 4I(I+1)J(J+1)}{8I(2I-1)J(2J-1)}], \quad (24)$$

where ν_J is the frequency (energy) of the state $n^{(2S+1)}L_J$ without the hyperfine interaction. In the above expression $A = \alpha/\hbar$ and $B = \beta/\hbar$ have units of Hz.

3.3 Rubidium Level Scheme

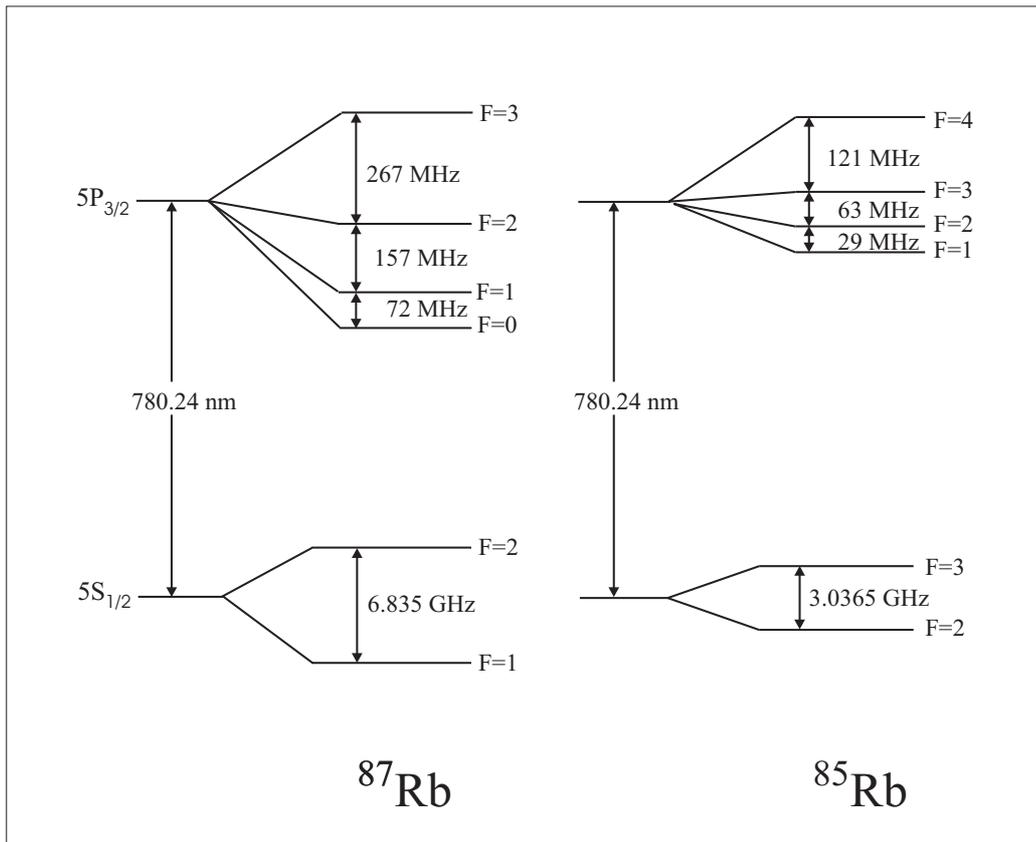It turns out that for the $5^2S_{1/2}$ ground state of both ^{85}Rb and ^{87}Rb, the last term in

Figure 6: Level scheme for the $5S_{1/2} \rightarrow 5P_{3/2}$ transition in [85]Rb and [87]Rb.

Eq.(24) is zero, and thus the hyperfine splitting in the ground state is characterized by a single parameter A($5^2S_{1/2}$), which for ^{87}Rb is $A(5^2S_{1/2}) = 3417.34$ MHz and for ^{85}Rb $A(5^2S_{1/2}) = 1011.91$ MHz. In contrast, for the first excited states $5^2P_{1/2}$ and $5^2P_{3/2}$ the hyperfine parameters A and B are both different from zero and typically on the order of a few tens of MHz, i.e. much smaller than for the ground state. Energy level diagrams of the states $5^2S_{1/2}$, $5^2P_{1/2}$ and $5^2P_{3/2}$ for both ^{85}Rb and ^{87}Rb are shown in Fig. 6. Exact values for A and B can be found in the literature (Ref.[3]).

It is the main goal of this experiment to measure the hyperfine constants (A,B) for the state $5^2P_{3/2}$ of the two isotopes of rubidium.

4 Experiment

4.1 Equipment and Layout

Laser

In the experiment, a home-built external cavity diode laser is used as a light source. The laser head contains a 780nm high-power AlGaAs semiconductor laser diode from Sharp (LTD025MD0) together with a collimating lens, mounted on a temperature-controlled stage. In addition, a diffraction grating provides feedback by acting as a wavelength selective mirror. The grating forms one end of the laser cavity and allows fine tuning of the laser's output frequency: the grating is mounted on a piezo which can be controlled by applying a high voltage. Besides, a change in diode temperature and/or diode current will also drastically(!) affect the output frequency (and power) of the laser. Hence, unless told otherwise, we strongly recommend not to touch the laser's current/temperature control unit (see Fig. 8). For more details on external cavity diode lasers see for instance Ref. [5].

Fig. 9 shows a photograph of an electronics rack containing two high-voltage boards ("HV-Rampe" and "Rampengenerator") and one small board with a summing amplifier circuit ("Adder"). With the "HV-Rampe" the laser's output frequency can be scanned. The three knobs of interest control the voltage ramp that is applied to the grating-piezo: the "Gain" knob determines the amplitude of the sweep, with the "Offset" knob the overall voltage offset can be adjusted and the ramp speed of the forward and backward ramps are controlled by the two potentiometers "Steilheit Rampe". With the "Int/Ext" switch, the voltage ramp can be completely switched off. The
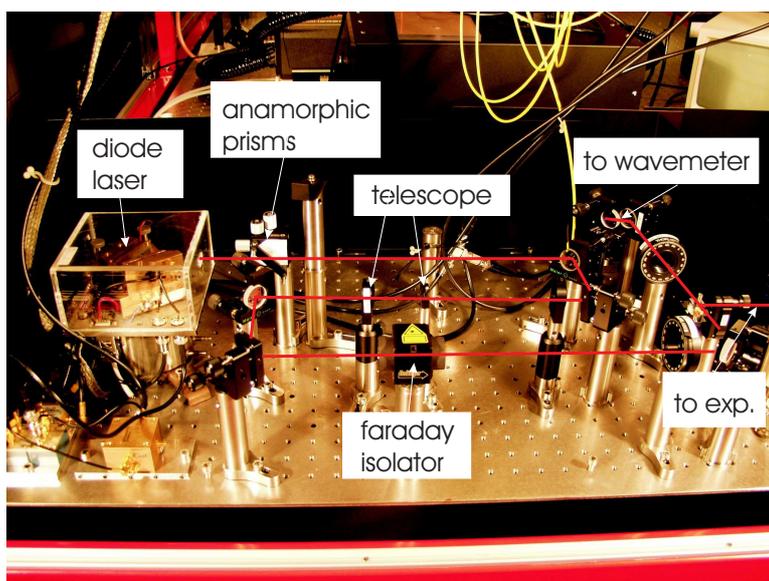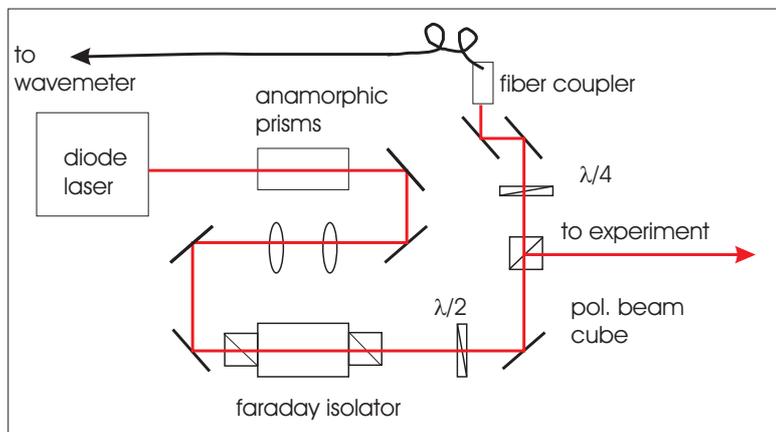
Figure 7: Home-built external cavity diode laser and some additional optics. Do not touch this part of the experiment. Miss-alignment can cause several hours of time delay!

Figure 8: Current and temperature controller for diode laser. Settings should not be changed.

"HV-Rampe" has two outputs, one delivering the high-voltage for the piezo, the other giving a TTL-level signal (0/+5V) which can be used to trigger the oscilloscope used for data acquisition. The switch "Trigger/Rampe" selects between a square pulse and a ramp. Note, that the high-voltage board "Rampengenerator" has exactly the same features.

Fabry-Perot Interferometer
The aim of this experiment is the determination of hyperfine constants (A,B). In order to extract quantitatively the energy splitting of the different hyperfine levels from measured spectra, a reference frequency is needed for calibration. Here, the Fabry-Perot interferometer comes into play. Such an interferometer consists of two highly-reflecting mirrors forming an optical cavity. For a given distance L between the mirrors, light is only transmitted through the cavity, if a standing wave can build up between the two mirrors, i.e. if an integer number n of half-wavelengths fit between the two mirrors. This condition yields the transmission frequencies of a Fabry-Perot as $\nu_n = nc/2L$. The frequency difference between two adjacent transmission
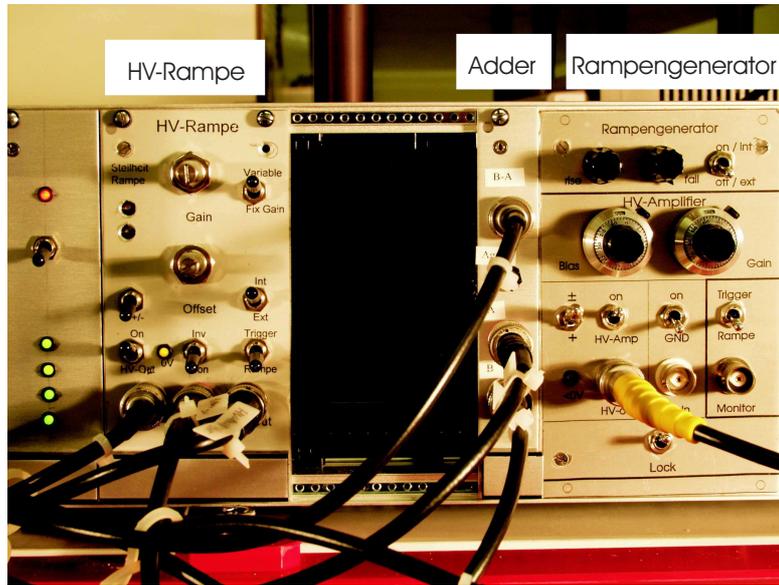
15

Figure 9: Rack with HV ramp for laser, summing amplifier and Fabry-Perot electronics.

peaks $c/2L$ is called the free spectral range. In the experiment, a Fabry-Perot with a free spectral range of 500 MHz is used.

The two Fabry-Perot mirrors are mounted on a piezo tube, such that their distance L, and therefore the transmission frequency, can be tuned by applying a high voltage to the piezo, which is controlled by the electronics board "Rampengenerator" mentioned before (see Fig. 9). The transmitted light is monitored with a photodiode that is connected to the oscilloscope.

Experimental Setup and Procedure

The experimental setup is shown in Fig. 10. The photograph and the corresponding schematic in Fig.7, show the home-built diode laser in its acrylic-glass housing. The elliptical light beam emitted from the laser is sent through an anamorphic prism pair, after which the beam is - to a good approximation - round in shape. Next, the beam passes through a telescope, which reduces the beam diameter to fit the aperture of the Faraday isolator. The Faraday isolator acts as the optical analogue of a normal diode: it prevents the beam from being reflected back into the laser. Such back reflections can lead to
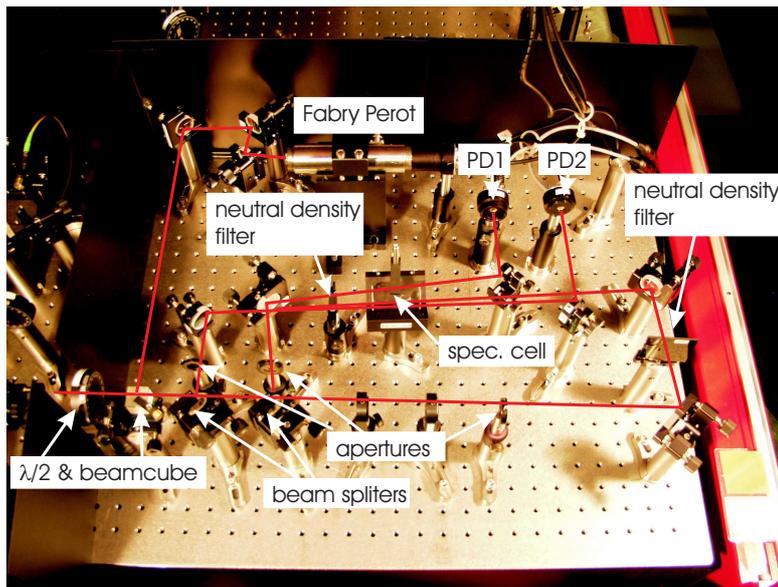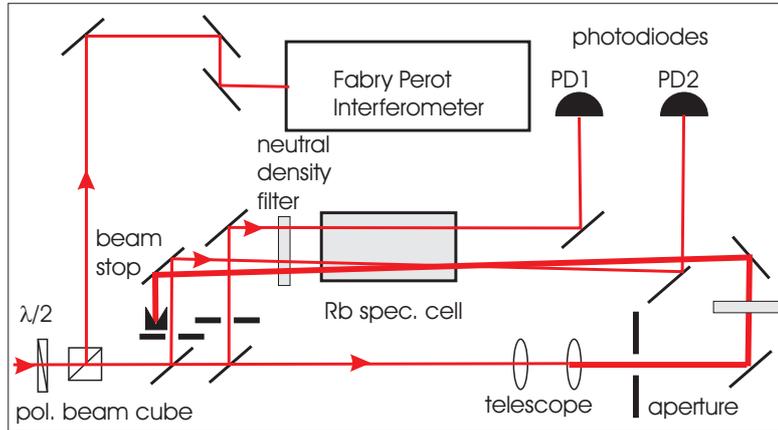
16

Figure 10: Experimental setup.

unstable behaviour of the laser. For more details on Faraday isolators, see for example [6]. The laser beam is then divided up by a combination of a $\lambda/2$-waveplate and a polarizing beam cube: the former rotates the (linear) polarization of the laser beam, whereas the latter's transmission is polarization dependent. For more detailed information on the working principles of polarization optics, see [7]. The position of the waveplate is chosen such that a small fraction of the laser power goes straight through the beam cube and into an optical fiber. The fiber is connected to a wavemeter in the lab next door, such that the laser wavelength can be monitored. The main part of the laser power is deflected by the beam cube and is available for the Doppler-free saturation spectroscopy.

The spectrocopy setup is shown in a photograph and a corresponding schematic in Fig. 10. There are two main beam lines. Again, a combination of a $\lambda/2$ waveplate and a polarizing beam cube splits the beam into two. The deflected beam goes directly into the Fabry-Perot interferometer and is already properly aligned. From the beam passing straight through the beam cube, three beams for saturation spectroscopy are derived. Two weak probe beams (one for reference purposes which will become clear later) are generated by inserting two $10:90$ beam splitters into the "high-power" (a few mW) pump beam. At each beam splitter two reflections, one coming from the back and one from the front facet, are generated. The weaker of the two is blocked using an aperture. In addition, the pump-beam diameter is controlled using a telescope and an aperture. The power in the pump and probe beams can be controlled by inserting neutral density filters. A set of filters covering about three orders of magnitude in attenuation is available. The three beams are directed through the rubidium vapour cell at the center of the table by highly reflecting mirrors (HR @780 nm). Unless told otherwise, you are not supposed to move or readjust the vapour cell!

In the beginning of the experiment, only the Fabry-Perot cavity (including the beam line), the vapour cell and the two photodiodes are mounted and should not be moved. Your task is it to set up the three beams for saturation spectroscopy. The following practical hints will help you:

- **First and most important of all: Be careful with the laser light! It can cause permanent damage to your and your partner's eyes. Always think about what you do in view of this danger! Wear your laser goggles!**

- Laser light at 780 nm lies in the near-infrared part of the spectrum. In a darkened room, however, light at 780 nm is visible and easily tracked with the help of a phosphorescent sensor card. Hence, switch off the room light! In addition, an infrared beam viewer is available.

- The standard beam height in all of our experiments is 5 inches (12.7 cm). Align the beams in that height (except for the reference probe beam; it passes the vapour cell above the other two beams).

- Before you start mounting the optics, think about how to best place **all** the components. As a reference, use the schematic in Fig. 10.

4.2   Alignment and Measurements

Fig. 11 shows three different absorption spectra that can be obtained with the suggested setup. For recording spectrum 2, the laser frequency was scanned and only one probe beam was going through the vapour cell. The other two beams were blocked. Thus, we get a normal Doppler-broadened absorption spectrum of a weak laser beam. The two peaks correspond to the transition $(^5S_{1/2}, F = 2 \rightarrow {}^5P_{3/2}, F = 1, 2, 3)$ in ^{87}Rb and to the transition $(^5S_{1/2}, F = 3 \rightarrow {}^5P_{3/2}, F = 2, 3, 4)$ in ^{85}Rb. When, in addition, the strong pump beam is passing through the cell, we get spectrum 3. Various Lamb dips, most of which are not fully resolved, appear. However, with only one probe beam present, the Doppler character remains. Next, the Doppler background can be removed by using the second probe beam, which should have no spatial overlap with the pump beam and basically shows an absorption signal like spectrum 2. Subtracting the signal generated by the second probe beam from spectrum 3, we obtain spectrum 4, where all the hyperfine transitions are individually resolved and no Doppler background is visible.

In order to remove the Doppler character completely and to obtain a flat baseline, careful alignment of the two probe beams is necessary. It is best to block the pump beam and align the two probe beams first. The signal from the two photodiodes PD1 and PD2 are subtracted from each other electronically. This is done on the electronics board "Adder" mentioned above (see Fig. 9). The gain for one of the signals can be adjusted with a potentiometer such that the difference signal is null throughout the whole frequency sweep of the diode laser. Then, introducing the pump beam crossing only one of the probe beams, produces saturated absorption lines on a flat background.
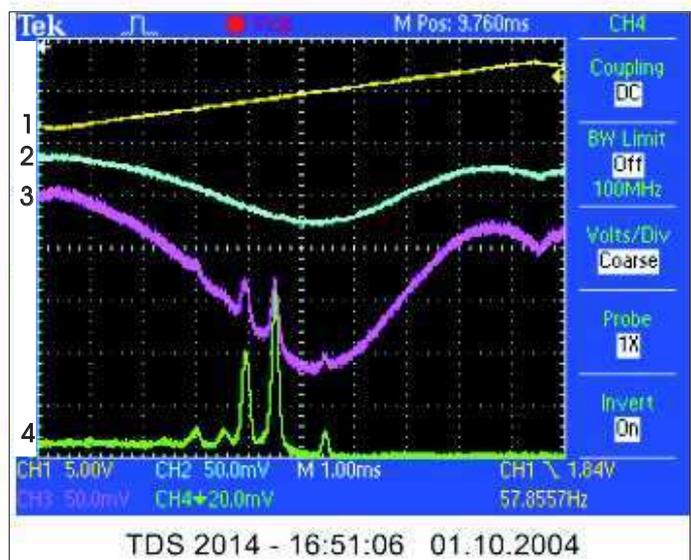
Figure 11: Oscilloscope screen shot. Yellow (1): Laser HV rampe. Blue (2): Signal of reference beam. Magenta (3): Photodiode signal of probe beam. Green (4): difference signal

Try to record spectra like the ones shown in Fig 11. To this end, try different combinations of pump and probe beam attenuation levels. Since the transition strenghts are different for ^{87}Rb and ^{85}Rb, best results are obtained when using different combinations of neutral density filters for the two isotopes.

Then, once you have the "best" combination of filters, quantitatively measure the frequency separation between the individual peaks in the spectrum by calibrating the time axis of the oscilloscope using the Fabry-Perot interferometer. For a given speed of the laser frequency ramp, you can directly read off the x-axis (time) separation between two different Fabry-Perot transmission peaks on the oscilloscope. (It is best to store the corresponding oscilloscope traces.) With the known free spectral range of the Fabry-Perot cavity, this x-axis separation directly translates into a frequency separation.

5 Analysis

- Using the level schemes in Fig. 6, assign a particular hyperfine transition to each of the lines in your recorded spectra. Matters are more complicated in the case of multilevel atoms compared to the two-level case. Therefore instead of three lines, you will find six spectral lines for each isotope. The additional three lines are called "cross-over resonances". For each pair of "normal" lines at frequencies ν_1 and ν_2, a cross-over resonance occurs at frequency $(\nu_1 + \nu_2)/2$.

- Find an explanation for these cross-over resonances and understand why they are so strong.

- From the measured line separations, determine a pair of hyperfine coupling constants (A,B) for each isotope. This can be done by subtracting Equation (24) from itself.

- Estimate the uncertainty in your results and compare your measured values for (A,B) to the accepted values in literature (see e.g. Ref. [3]).

References

[1] T. W. Hänsch, A. L. Schawlow, and G. W. Series. The spectrum of atomic hydrogen. *Scientific American*, 240:72, 1979.

[2] W. Demtröder. *Laserspektroskopie.* Springer, Heidelberg, 1991.

[3] E. Arimondo, M. Inguscio, and P. Violino. Experimental determinations of the hyperfine structure in the alkali atoms. *Rev. Mod. Phys.*, 49:31, 1977.

[4] P. W. Milonni and J. H. Eberly. *Lasers.* Wiley-Interscience, New York, 1988.

[5] P. Zorabedian. Tunable external-cavity semiconductor lasers. In F. J. Duarte, editor, *Tunable Lasers*, pages 349–442. Academic Press, London, 1995.

[6] L. Bergmann and C. Schäfer. *Lehrbuch der Experimentalphysik, Band 3, Optik.* de Gruyter, Berlin, 1993.

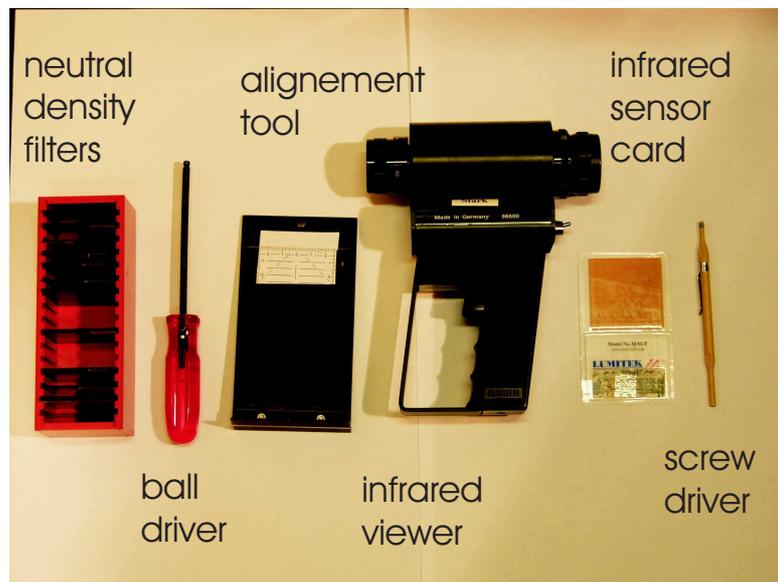[7] W. Demtröder. *Experimentalphysik 2.* Springer, Berlin, 2002.

A   Tools

Figure 12: Important tools for setting up the experiment.